Trails of the killer tsunami: A preliminary assessment using satellite remote sensing technique

Tsoo-nah-mee, the Japanese word meaning harbour wave is basically a wave train, generated in the ocean due to sudden disturbance that vertically displaces the water column. The causative factor of such an impulse can be ocean-floor tectonics (earthquakes and volcanic eruptions) or mass movements in the continental slope. All these processes result in elevating (potential energy) the water column up above the mean sea level, which then horizontally propagates (kinetic energy) as tsunami. Thus the tsunami differs from the tidal wave in that the latter has very low-order energy, since it originates due to gravitational forces.

The tsunami once generated, is split into distant (propagating towards ocean) and local (propagating towards nearby coast) tsunamis which travel in opposite directions with an amplitude about half of the original. Both tsunamis have a wavelength more than 100 km and period of the order of about 1 h. Since the speed of the tsunami varies as the square root of water depth, it travels faster in the open ocean than near the coast[1]. As the tsunami moves from the deep ocean to the shore, its amplitude increases and wavelength decreases. This results in the steepening of the tsunami run-up, a measure of the height of the water on shore[2]. After hitting the shore, a part of the tsunami energy is reflected back to the open ocean and also results in generation of edge waves that travel back and forth parallel to the shore. The generation of run-up and edge waves is complex depending upon the slope, smoothness, wave type, depth of water and coastal topography[2–4].

The recent tsunami that paralysed the entire southeast and southern parts of India, owes it origin to a devastative earthquake off the west coast of Sumatra (5.51°N 92.92°E) with a magnitude of 8.9 on the Richter scale and focus[5] at a depth of 33.9 km. Here an attempt has been made to understand the trails of the recent tsunami during its propagation and aftermath using satellite remote sensing and GIS techniques.

The adopted methodology includes a three-phased approach, viz.

1. Acquisition of MODIS – Terra and Aqua calibrated radiance data sets (level 1B) of 25 December 2004 (07 : 30 GMT) and 26 December 2004 (5 : 10, 5 : 20, 8 : 15GMT). MODIS band 1 (0.62–0.67 μm) and band 2 (0.841–0.876 μm) (250 m spatial resolution) are used to map coastal flooding. Band 3 (0.459–0.479 μm) and band 4 (0.545–0.565 μm) have spatial resolutions of 500 m. For sediment load study, band 2 was resampled to 500 m. As MODIS-Terra data was acquired less than 3 h after the earthquake, special emphasis is made to understand the trails during the propagation and after its impact on the coast.
2. The raster data preparation and image analyses were carried out using ERDAS-imagine (ver. 8.5) following the standard image processing procedures[6]. Precise image-to-image registration was achieved between pre- and post-event datasets by way of selecting about 60 ground control points (GCP) in a second order polynomial equation. By this way, the root mean square error was restricted to 0.05. The post-event data is normalized to pre-event data by fitting linear regression equation. Principal component analysis and band ratios are derived to document the moisture changes (on land) and suspended sediment concentration (in ocean).
3. Mapping the tsunami-affected areas using NDVI ratios. Vector layer of the inundated area was generated using ARC/Info ver. 7.1.1. The inundated area statistics was computed from this layer.

Since MODIS has 250 m spatial resolution in band 1 and band 2, these two bands are

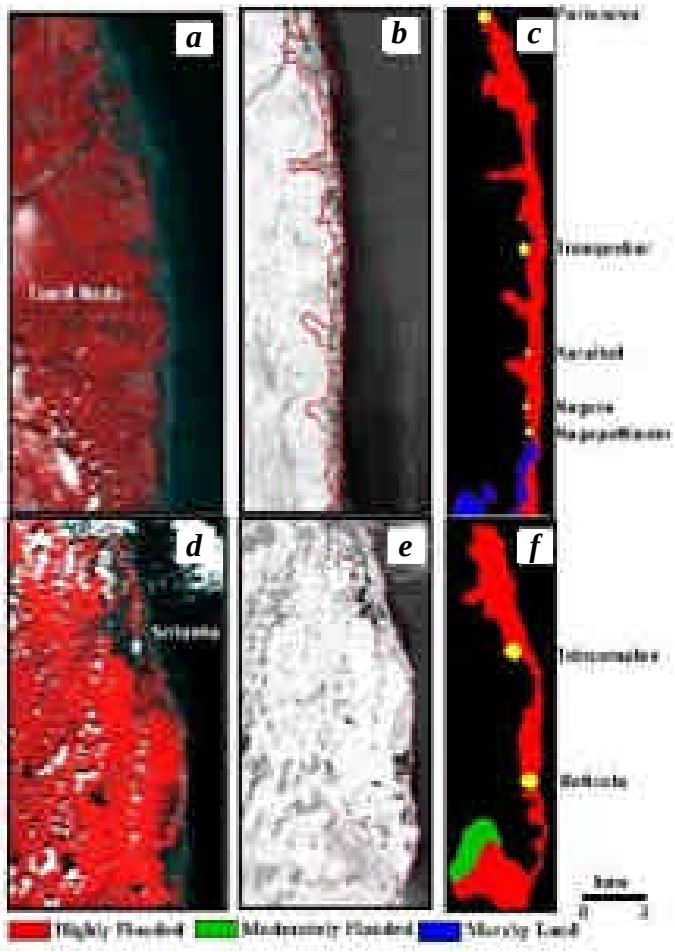

Figure 1. Post-event images showing the impact in the tsunami-hit areas. FCC (R : G : B, 2 : 1 : 1) of coastal Tamil Nadu (***a***) and Eastern Sri Lanka (***d***). NDVI maps showing coastal inundation (***b*** and ***e***). Vector layers (***c*** and ***f***) showing extent of flooding and locations of the affected areas.

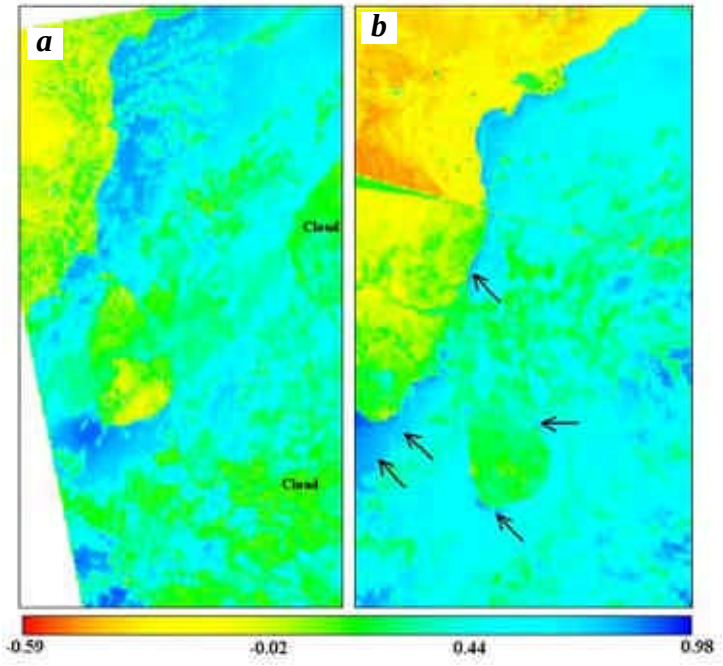

Figure 2. Pre- (***a***) and post- (***b***) band ratio maps (b4 and b2) depicting the changes in suspended sediment concentration in coastal waters.

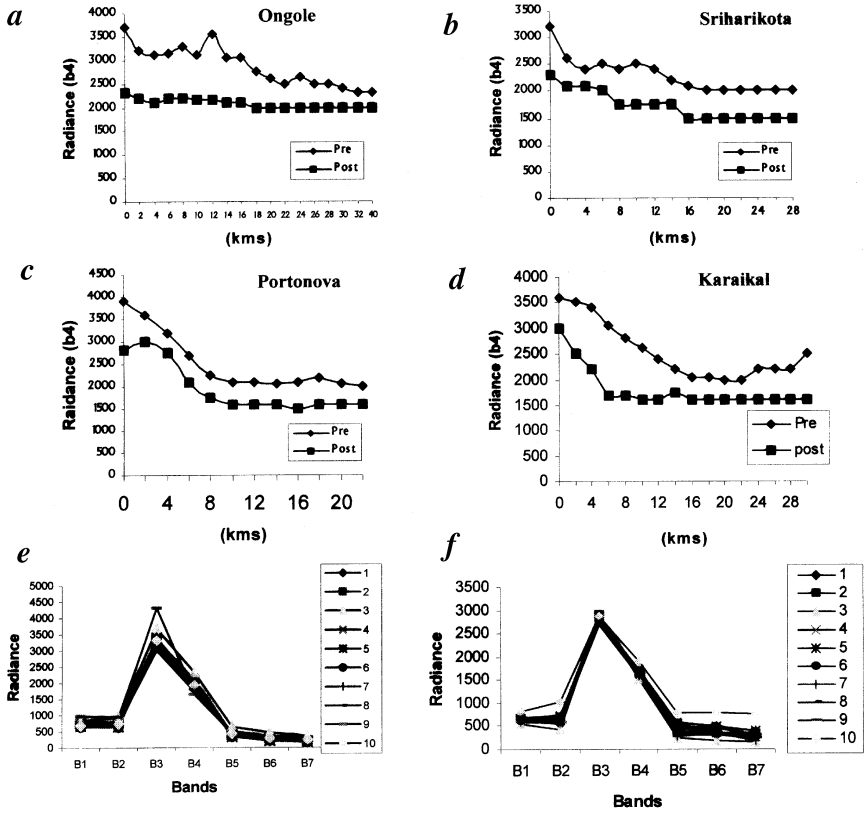

Figure 3 ***a–d.*** Spatial profile of pre- and post-event radiances ($mWcm^{-2}sr^{-1}\mu m^{-1}$) of band 4 depicting the changes in suspended sediment load. Spectral profile (b1–b7) depicting the changes in pre- (***e***) and post-event (***f***) changes in radiance values. (Series 1–10 are mean values of radiances from representative samples off Ongole, Sriharikota, Chennai, Portonova, Karaikal, Nagore, Kanyakumari, and Colombo coasts).

used to derive NDVI for better mapping accuracy. As NDVI is sensitive to moisture changes[7,8], it was efficiently used to map the inundated areas due to wave action (Figure 1). The NDVI values of the post-event data of the affected coastal area vary from –0.18 to 0.7, whereas in the case of pre-event data it varies from 0.25 to 0.80. Negative NDVI values represent highly moist or flooded areas. It is evident from the results that the worst affected areas are mainly between Baticola (Sri Lanka) in the south to Pulicot lake (India) in the north. The extent of coastal flooding derived on this basis varies from 0.5 km to 3.0 km (Nagapattinam, Nagore, Karaikal, Tranquebar and Portonova). However, in the case of marshy areas, the impact due to wave run-up could not be estimated. An area of 706 km^2 was worst affected between Nagapattinam and Pulicot lake, of which 282 km^2 lies between Nagapattinam and Portonova.

Since high quantum of energy is dissipated by the wave in the shallow waters, tsunami churns the shallow water sediments and thereby increases the sediment load[9]. Suspended sediment concentration (SSC) and sensor measured radiance (L_I) have a strong curvilinear relation[10,11]. Sediment load from excess reflectance at bands 2, 3 and 4 beyond the power law values[12] are considered for this work. Radiance values of MODIS in channels 2 and 4 are used to evaluate the changes in sediment load. For coastal waters, the blue channel (0.47 μm) is not suitable for sediment analysis because it is more sensitive to atmospheric scattering as well as strong absorption due to yellow substances. Similarly, water-leaving radiance for bands at higher wavelengths (0.86–2.13 μm) is assumed to be zero because of high absorption by water. Hence, the reflectance at these wavelengths is contributed mainly by atmosphere. Thus, the measurements at 0.545–0.565 μm are influenced mainly by sediments and to a lesser extent by the aerosol. The ratios between bands 4 & 2 (band 4–band 2/band 4 + band 2) is more sensitive to sediment load since it minimizes the atmospheric effects. The ratio has an inverse relation with the sediment load. Since the present study is confined to identification of changes in SSC between the pre- and post-event, calibrated radiances alone were used.

Figure 2 compares the band ratio for 25 December 2004 (7 : 30 GMT) and 26 December 2004 (5 : 10, 5 : 15 and 8 : 15 GMT) datasets. In the post-event datasets, there is decrease in ratio values (mode = 0.43) compared to the pre-event (mode = 0.77)

in the coastal waters. However, in the inland water bodies, this trend is not observed (pre- and post-mode, 0.70 and 0.72 respectively). This could be attributed mainly to increase in sediment load along the coastal waters. The spatial profile of radiance (band 4) from the coast to ocean (Figure 3 *a–d*) showed clear stratification of turbid water in the pre-event, which became less apparent after the event. This suggests a strong turbulence and mixing in the near coastal water due to impinging of tsunami. Spectral profile of radiance (Figure 3 *e*, *f*) from representative samples off Ongole to Colombo coast indicates that the post-event data showed a decrease in the radiance in all wavelengths. This may be attributed to change in sediment type[13] and rise in water column depth on 26th data due to wave run-up and associated effects[14].

To conclude, the effects of this devastating tsunami were noticed 3 km on land to 40 km on the ocean. The worst affected area stretch from Baticola (Sri Lanka) to Portonova (India). After the tsunami event, SSC stratification in coastal waters became less prominent. The decrease in radiance of coastal waters after the tsunami event can be attributed to increase in water depth and changes in sediment type. Even though this study brings out some of the impacts of tsunami, data of high spatial resolution is needed to accurately estimate the coastal flooding. To arrive at finer details of sediment load, turbulence and mixing, precise atmospheric correction of the satellite data is needed. Some of the affected areas could not be studied because of cloud cover.

1. Abe, K. and Ishil, H., *J. Phys. Earth*, 1980, **28**, 543–552.
2. Kanoglu, U. and Synolakis, C. E., *J. Fluid Mech.*, 1998, **374**, 1–28.
3. Hughes, S. A., *Coast. Eng.*, 2004, **51**, 1085–1104.
4. Li, Y. and Raichlen, F., *J. Fluid Mech.*, 2002, **456**, 295–318.
5. http//neic.usgs.gov/neis/bulletin/bulletin.html
6. Jensen, J. R., *Introductory Digital Image Processing: A Remote Sensing Perspective*, Prentice Hall, New Jersey, 1995, p. 316.
7. Townshend, J. R. G. and Justice, C. O., *Int. J. Rem. Sen.*, 1986, **7**, 1435–1445.
8. Wang, C., Qi, J., Moran, S. and Marsett, R., *Remote Sensing Environ.*, 2004, **90**, 178–189.
9. Kobayashi, N. and Karjadi, E. A., *J. Waterway Port Coastal Ocean Engg. ASCE*, 1994, **120**, 56–73.
10. Ritchie, J. C. and Cooper, C. M., *Int. J. Remote Sensing*, 1988, **9**, 379–387.
11. Ritchie, J. C., Schiebe, F. R. and McHenry, J. R., *Photogramm. Eng. Remote Sensing*, 1976, **42**, 1539–1545.
12. Li, R. R., Kaufman, Y. J., Gao, B.-C. and Davis, C. O., *IEEE Trans. Geosci. Remote Sensing*, 2003, **41**, 559.
13. Novo, E. M. M., Hansom, J. D. and Curran, P. J., *Int. J. Remote Sensing*, 1989, **10**, 1283–1289.
14. Toole, D. A., Siegel, D. A., Menzies, D. W., Neumann, M. J. and Smith, R. C., *Appl. Opt.*, 2000, **39**, 456–469.

ACKNOWLEDGEMENTS. We thank NASA for keeping the data on their portal. We also thank Dr Shailesh Nayak, SAC, Ahmedabad and the referee for valuable comments.

Received 15 January 2005; revised accepted 17 February 2005

D. RAMAKRISHNAN[1,*]
S. K. GHOSH[2]
V. K. M. RAJA[1]
R. VINU CHANDRAN[1]
A. JEYRAM[1]

[1]*Regional Remote Sensing Service Centre, Indian Space Research Organization, Indian Institute of Technology Campus, Kharagpur 721 302, India*
[2]*School of Information Technology, Indian Institute of Technology, Kharagpur 721 302, India*
**For correspondence.*
e-mail: aarkay_geol@yahoo.com